Seventh International Conference on CFD in the Minerals and Process Industries
CSIRO, Melbourne, Australia
9-11 December 2009

A CFD MODEL FOR SIMULATING HIGH PRESSURE THERMAL (HPT) PROCESSING – IMPACT OF MATERIAL PROPERTIES AND PROCESSING CONDITIONS ON PREDICTION ACCURACY

Kai KNOERZER and Cornelis VERSTEEG

Innovative Foods Centre, CSIRO Food and Nutritional Sciences, Private Bag 16, Werribee, Victoria, Australia
*Corresponding author, E-mail address: kai.knoerzer@csiro.au

ABSTRACT

High pressure in combination with heat is effective for microbial spore inactivation. It has the potential to deliver novel shelf stable food products with superior sensory properties, particularly compared to retorted products. The combined process enables sterilisation at reduced temperatures and/or shorter processing times compared to heat alone. A major challenge is to achieve temperature uniformity inside the vessel as the fast temperature rise upon pressurisation can be partially lost to the cooler vessel walls, resulting in an ineffective non-uniform process. CFD modelling can provide a representation of flow and temperature profiles during the HPT process, which is important for evaluating process performance and effective optimisation. However, it is essential that the CFD models are validated and predictions agree very well with temperatures measured in actual processes.

The objective of this research was to study the impact of variations in simulated process conditions and compression fluid properties, such as compression heating coefficients, on the prediction accuracy of a CFD model for a Stansted 3.6L Isolab HPTS system. Model development and simulations were performed using COMSOL Multiphysics™.

Good agreement was found between simulated and measured temperature distributions when actual pressure profiles (impacting not only on pressure evolution, but also on fluid inlet velocity and time-temperature profile), and accurate properties for the compressed material were used. Inaccurate approximations of these conditions and values resulted in much less useful models.

NOMENCLATURE

C_P	*Specific heat capacity*	*J/(kgK)*
C_μ	*Constant*	m^4/kg^4
g	*Gravity constant*	$9.81\ m/s^2$
k	*Turbulent kinetic energy*	kg^2/K^2
k_l	*Thermal conductivity*	*W/(m·K)*
k_T	*Turbulent thermal conductivity*	*W/(m·K)*
P	*Pressure*	*Pa, MPa*
Q	*Volumetric compression heating rate*	W/m^3
r	*Horizontal position (radial direction)*	*m*
T	*Temperature*	*°C or K*
t	*Time*	*s*
$\vec{v}$	*Velocity vector*	*m/s*

Greek symbols

α_P	*Thermal expansion coefficient*	K^{-1}
ε	*Dissipation rate of turbulence energy*	m^2/K^3
η_T	*Turbulent viscosity*	*kg/(m·K)*
η	*Dynamic viscosity*	*Pa·s*
ρ	*Density*	kg/m^3

Abbreviations

CFD	*Computational Fluid Dynamics*
FEM	*Finite Element Method*
HP	*High Pressure*
HPT	*High Pressure Thermal*
PG	*Propylene-Glycol*

Operator

d	*Differential*
∂	*Partial differential*
∇	*Nabla operator (vector differential operator)*

INTRODUCTION

High pressure thermal (HPT) processing is an investigated and proposed technology for high-temperature short-time commercial sterilisation of chill- and ambient stable low-acid food products. Commencing with moderate initial product and pressure chamber temperatures of 60 to 90°C, HPT processing currently employs pressures of up to 700 MPa to increase the temperature of the preheated food to inactivate bacterial spores (Margosch et al., 2004; Bull et al., 2009). Temperature increase during pressurisation is induced by compressive work against intermolecular forces and assuming that there are no thermal losses, the temperature reached during pressurisation can be readily derived (Knoerzer et al., 2010; Knoerzer et al., 2007; Juliano et al., 2009):

$$\frac{dT}{dP} = \frac{\alpha_p(P,T)}{\rho(P,T)\cdot C_p(P,T)}\cdot T \qquad (1)$$

Where T denotes the absolute temperature in *K*, P the pressure in *Pa*, α_P the thermal expansion coefficient in K^{-1}, ρ the density in kg/m^3 and C_P the specific heat capacity in *J/kgK*.

Product and compression fluid temperatures may rise up to 40°C during high-pressure treatment, depending on the initial temperature, target pressure, and compression heating properties of the compressed material.

The pressure profile, as well as the compression heating properties used in the modelled scenario, impact hereby directly and potentially significantly on the prediction outcomes.

The objective of this work was to quantify this impact and compare predictions of models with accurate conditions and material properties with modelled scenarios where simplified processing conditions and estimated material properties were used.

MODEL DESCRIPTION

The HPT model was designed to be a good approximation of a Stansted ISO-LAB FPG11501 HPP 3.6 L (see figure 1).

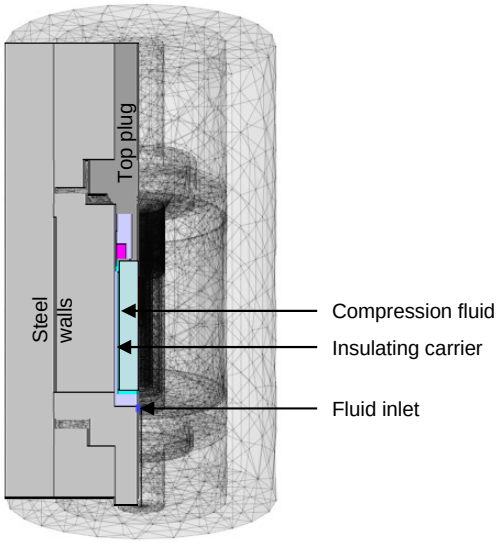

Figure 1: Configuration of model geometry comprising the steel components of the vessel, the insulated carrier (Polypropylene), the compression medium domain and the fluid inlet.

An axis-symmetric model was developed, as the actual system comprises mainly axis-symmetric features.

The modelling was performed in COMSOL Multiphysics™, using two application modes: (i) the *k-ε* Turbulence model, applied to the compression medium domain only (inactive at the solid regions occupied by the carrier), and (ii) the general heat transfer model, applied in both liquid and solid regions.

Governing equations:

The thermo- and fluid-dynamic behaviour of the pressure medium is described by conservation equations of mass (Equation 2), momentum and energy (Chen, 2006).

$$\frac{\partial \rho}{\partial t} + \nabla \cdot \left(\rho \vec{v}\right) = 0 \qquad (2)$$

Where ρ is the density as function of pressure and temperature and $\vec{v}$ is the velocity vector.

The inflowing pressurisation medium enters through the high pressure system inlet at a high velocity, creating turbulent flow in the bottom region. Turbulence was solved by applying the *k-ε* model that included an additional "turbulence viscosity" and "turbulent thermal conductivity" in the equations for conservation of momentum and energy, respectively, to take the contributions of turbulent eddies into account (Nicolaï et al., 2007; COMSOL Multiphysics, 2006). The turbulent viscosity η_T is given by:

$$\eta_T = \rho C_\mu \frac{k^2}{\varepsilon} \qquad (3)$$

where C_μ =0.09 (Launder and Spalding, 1974), k is the turbulent kinetic energy and ε the dissipation rate of turbulence. Here, the momentum equation (extended according to COMSOL Multiphysics (2006)) gives the following expression:

$$\rho\left[\frac{\partial \vec{v}}{\partial t} + \left(\vec{v} \cdot \nabla\right)\vec{v}\right] = -\nabla P + \nabla \cdot \left((\eta + \eta_T) \cdot \nabla \vec{v}\right) + \rho g \qquad (4)$$

Where $\vec{v}$ denotes the average velocity, P is the pressure, η represents the dynamic viscosity of the compressed fluid, and g represents the gravity constant. In addition to the continuity equation, the *k-ε* closure includes two extra transport equations solved for both k and ε using empirical model constants (COMSOL Multiphysics, 2006).

The *k-ε* closure equations were coupled with the energy conservation equation for heat transfer through convection and conduction, assuming non-isothermal flow. This equation was modified (from Kowalczyk et al. (2004) and extended according to COMSOL Multiphysics (2006)) by including the turbulent thermal conductivity k_T (with $k_T = C_P \cdot \eta_T / Pr_T$):

$$\rho C_p \left(\frac{\partial T}{\partial t} + \vec{v} \cdot \nabla T\right) = Q + \nabla \cdot \left((k_1 + k_T)\nabla T\right) \qquad (5)$$

where k_1 is the thermal conductivity, and C_p is the specific heat capacity. Pr_T is the turbulent Prandtl number. The source term Q arises from compression, by rewriting equation 1:

$$Q = T\alpha_P \frac{dP}{dt} \qquad (6)$$

Process conditions:

Two pressure profiles were studied (see figure 2). Firstly, a simple pressure profile, derived from the pressure come-up, holding and decompression times from the measured pressure profile and a target pressure of 600 MPa, was used. The compression and decompression was hereby approximated linearly. Subsequently, a real and accurate, but more complicated pressure profile from an actual high pressure experiment was selected.

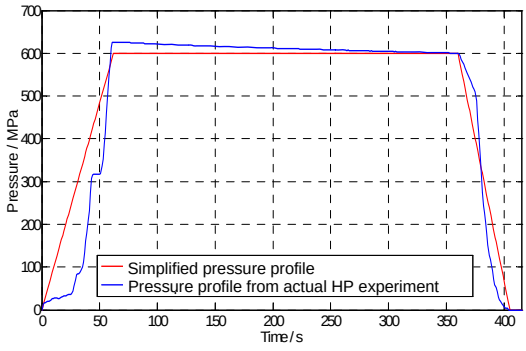

Figure 2: Pressure profiles used in the simulated high pressure scenarios.

Based on the two pressure profiles, the velocity at the inlet was estimated based on the density change during the pressure cycles.

Boundary conditions:

Fluid-solid boundaries had to be defined for the *k-ε* Turbulence mode on the liquid domain, whereas thermal boundaries were defined for the general heat transfer mode for all domains. Symmetry boundary conditions on the axis ($r = 0$) were assumed.

An inflow (and outflow) velocity boundary condition was defined for the inlet/outlet tube based on the pressure profiles used in the respective scenarios. I.e. the changes in pressure lead to changes in density which in turn dictate fluid motion following equation 2.

A logarithmic wall function condition as described by (Knoerzer et al., 2007; Knoerzer et al., 2009a) was assumed at the interior vessel and carrier walls.

The inlet boundary was set to a constant temperature throughout the process and was estimated to be at 80ºC. Upon pressure release, the tube becomes an outlet with a convective flux boundary condition.

Continuity of heat flux is assumed at all fluid-solid and solid-solid boundaries. Whereas the heat flux from the steel to the surrounding air is dictated by free convection with a heat transfer coefficient of 5 W/m^2K and an external temperature of 30°C.

More information on the boundary conditions used can be found in Knoerzer et al. (2009a), where a pilot-scale high pressure system was modelled.

Material Properties:

Physical properties, including expansion coefficient, density, specific heat capacity, thermal conductivity and viscosity of the compression medium and their variation with pressure and temperature were used in the liquid domain of the model. Two scenarios were investigated: (i) Scenario 1 used the compression heating properties of pure water, (ii) Scenario 2 was based on the compression heating properties of the actual medium, a 40% propylene-glycol/water mixture, used in the experiments. The propylene-glycol/water properties were obtained from separate investigations (Knoerzer et al., 2009)

Properties for Polypropylene and steel were taken as constants from the COMSOL database, independent of temperature and pressure variations. The expansion coefficients, and therefore compression heating, of the steel were assumed to be zero. The compression heating properties of the polypropylene as determined in a separate study (Knoerzer et al., 2009b), were included in the model.

Computational Methods:

The partial differential equations describing the model were solved with the finite element method (FEM). A commercial software package, COMSOL Multiphysics™ (COMSOL AB, Stockholm, Sweden) was used, incorporating toolboxes for simultaneously solving multiphysics problems. The axis-symmetric geometry was discretised by triangular mesh elements. The mesh consisted of approximately 10,000 elements. Computations were carried out on a workstation running the 64bit OS Windows 2003 server. Two dual-core processors (each 2.33 GHz) and 20 GB RAM allowed for solving the models within approximately 45 minutes of computation time.

RESULTS

The CFD model predicts the transient temperature and flow distributions throughout the simulated geometry. Figure 3 shows the temperature distribution in an axis-symmetric plane at the end of pressure hold time for the model, based on the measured pressure profile and the material properties of the propylene-glycol/water mixture. Also indicated is the flow profile at this stage of the process (arrows).

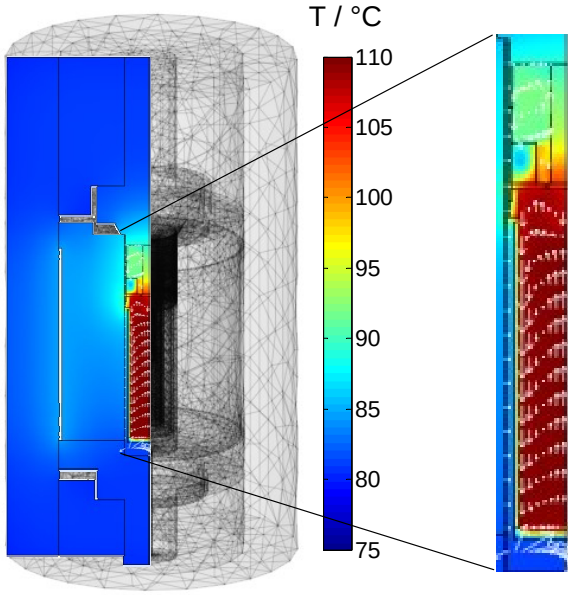

Figure 3: Flow and temperature distribution inside the Stansted 3.6 L HPT unit at the end of pressure hold time.

The predicted transient temperature evolution in the system, based on the different scenarios, was compared to thermocouple measurements.

Impact of process conditions (pressure profiles)

Figure 4 shows the predicted temperature profiles in a discrete location (highlighted in figure 4a) inside the insulating carrier; the compression fluid in these scenarios was the propyleneglycol/water mixture. Predictions based on the pressure profile from the actual experiment show pronounced differences to the predictions based on the initially used simplified pressure profile (figure 4b). A good agreement with measurements was found when actual process conditions were used (figure 4c, parity plot, $R^2 = 0.99$), whereas relatively poor agreement was found for the simulations with the simplified pressure profile ($R^2 = 0.88$).

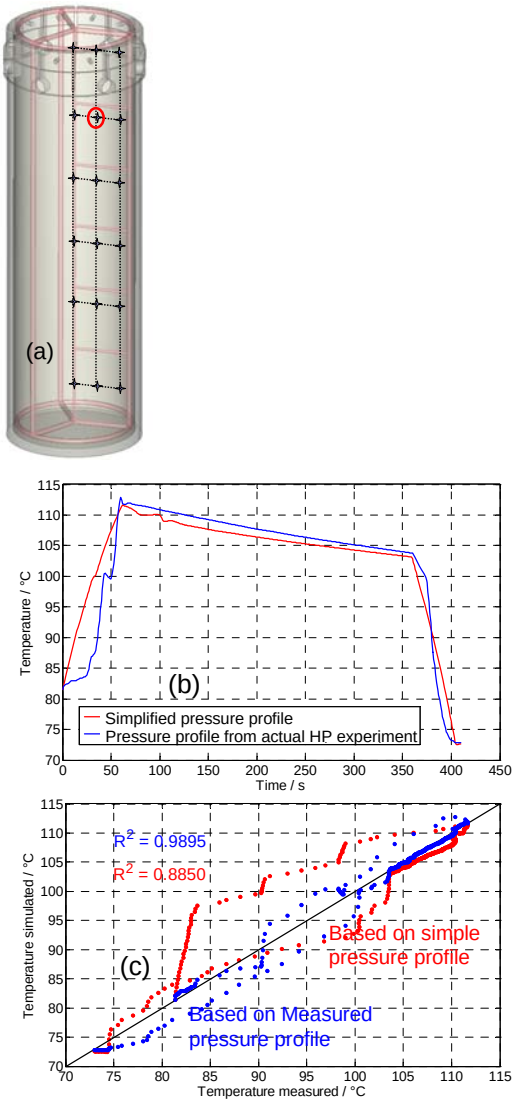

Figure 4: (a) Insulating carrier; location for comparison highlighted (red circle)

(b) Predictions based on the two modelled scenarios

(c) Parity plot for comparison with measured data

Impact of material properties (compression heating coefficients)

Figure 5 shows the predicted (using water properties and properties of the actual mixture) and measured temperature profiles in the same location in the insulating carrier (figure 4a). As can be seen, a good agreement with measurements was found when the compression heating properties of the actual glycol/water mixture were used (figure 5 a and b, R^2 = 0.98, during holding time). Using the compression heating properties of pure water however, gives only poor agreement with the measurements (R^2 = 0.03, during pressure holding).

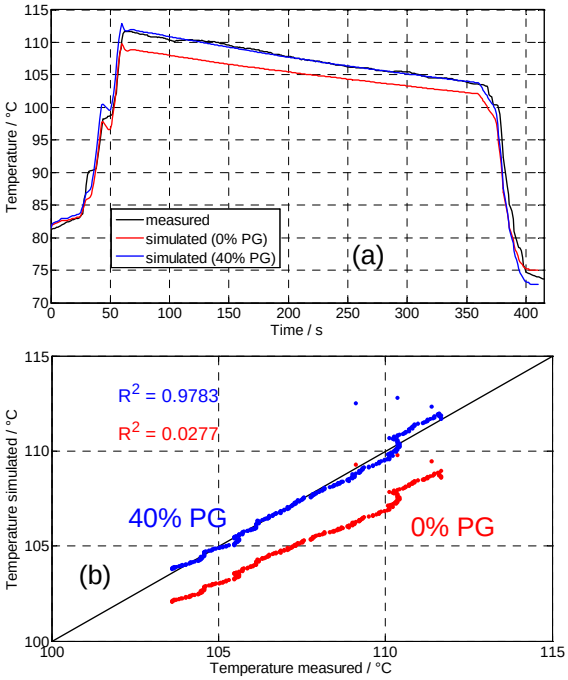

Figure 5: (b) Measured and predicted (based on the two modelled scenarios, i.e. water properties and glycol/water properties) temperature profiles/

(c) Parity plot (of data during hold time) for comparison with measured data

CONCLUSION

A CFD model of a HPT process was presented and the critical importance of accurate processing conditions and material properties for realistic results was shown. For successful modelling of HPT processing, material properties with their functional dependence with pressure and temperature must be implemented in the model for the fluid used in the actual process in order to achieve good agreement with actual measurements. Unfortunately, thermophysical properties as functions of pressure and temperature for most food products, carrier materials and compression liquids are unknown and need to be determined as well. Furthermore, also the processing conditions, here the pressure profile, has to be as close to the real pressure profiles as possible to get meaningful and accurate results. The CFD model, comprising actual material properties and pressure profiles, was validated based on thermocouple measurements. A very good agreement was found for the predicted temperature profiles in an axis-symmetric plane inside the insulating product carrier.

With CFD models like this, it is possible to develop and optimise equipment, e.g. for the product carrier, its geometry and material, as well as the processing conditions. Such specifically designed and optimised systems then provide uniform treatment, essential for using the technology to deliver shelf stable low acid food products without food safety risks or significant over processing. A further enhancement of the model allows for coupling the predicted temperature distributions with bacterial spore inactivation kinetics, yielding inactivation distributions for specific target organisms.

REFERENCES

BULL, M.K., OLIVIER, S.A., and CHAPMAN, B. (2009). Synergistic inactivation of *Clostridium botulinum* spores by high pressure and heat is strain and product dependent, Applied and Environmental Microbiology, 75(2), 434-445.

CHEN, X.D. (2006). Modeling thermal processing using computational fluid dynamics (CFD), Sun, D.W. (Eds.), Thermal food processing, (5), 133-151, Boca Raton, Taylor & Francis, Series: Thermal Food Processing: New Technologies and Quality Issues, Food Science and Technology.

COMSOL MULTIPHYSICS. (2006). Chemical Engineering Module, Stockholm, Sweden, COMSOL AB.

JULIANO, P., KNOERZER, K., FRYER, P., and VERSTEEG, C. (2009). C. botulinum inactivation kinetics implemented in a computational model of a high pressure sterilization process., Biotechnology Progress, 25(1), 163-175.

KNOERZER, K., BUCKOW, R., JULIANO, P., CHAPMAN, B., and VERSTEEG, C. (2009a). Carrier optimisation in a pilot-scale high pressure sterilisation plant – An iterative CFD approach, Journal of Food Engineering, (available online, DOI: 10.1016/j.jfoodeng.2009.10.010).

KNOERZER, K., BUCKOW, R., SANGUANSRI, P., and VERSTEEG, C. (2010). Adiabatic Compression Heating Coefficients for High Pressure Processing of Water, Propylene Glycol and Mixtures – A Combined Experimental and Numerical Approach, Journal of Food Engineering, 96, 229-238.

KNOERZER, K., BUCKOW, R., and VERSTEEG, C. (2009b). Adiabatic compression heating coefficients for high pressure processing – A study of some insulating polymer materials, Journal of Food Engineering, (submitted August 2009).

KNOERZER, K., JULIANO, P., GLADMAN, S., VERSTEEG, C., and FRYER, P. (2007). A Computational Model For Temperature and Sterility Distributions in a Pilot-Scale High-Pressure High-temperature Process, Aiche Journal, 53(11), 2996-3010.

KOWALCZYK, W., HARTMANN, C., and DELGADO, A. (2004). Modelling and numerical simulation of convection driven high pressure induced phase changes, International Journal of Heat and Mass Transfer, 47(5), 1079-1089.

LAUNDER, B.E. and SPALDING, D.B. (1974). The numerical computation of turbulent flows, Computer Methods in Applied Mechanics and Engineering, 3(2), 269-289.

MARGOSCH, D., EHRMANN, M.A., GANZLE, M.G., and VOGEL, R.F. (2004). Comparison of pressure and heat resistance of Clostridium botulinum and other endospores in mashed carrots, Journal of Food Protection, 67(11), 2530-2537.

NICOLAI, B.M., VERBOYEN, P., and SCHEERLINCK, N. (2007). Modeling and simulation of thermal processes, Richardson, P. (Eds.), Thermal technologies in food processing, 91-112, Boca Raton, FL, CRC Press.